Doctoral Program
Computational Mathematics
Numerical Analysis and Symbolic Computation

Bases and dimensions of bivariate hierarchical tensor–product splines

Carlotta Giannelli Bert Jüttler

DK-Report No. 2011-11 10 2011

A–4040 LINZ, ALTENBERGERSTRASSE 69, AUSTRIA

Supported by
Austrian Science Fund (FWF) Upper Austria

Editorial Board: Bruno Buchberger
Bert Jüttler
Ulrich Langer
Esther Klann
Peter Paule
Clemens Pechstein
Veronika Pillwein
Ronny Ramlau
Josef Schicho
Wolfgang Schreiner
Franz Winkler
Walter Zulehner

Managing Editor: Veronika Pillwein

Communicated by: Ulrich Langer
Josef Schicho

DK sponsors:

- **Johannes Kepler University Linz** (JKU)
- **Austrian Science Fund** (FWF)
- **Upper Austria**

Bases and dimensions of bivariate hierarchical tensor–product splines

Carlotta Giannelli*, Bert Jüttler†

Institute of Applied Geometry, Johannes Kepler University, Altenberger Str. 69, 4040 Linz, Austria

Abstract

We prove that the dimension of bivariate spline spaces of degree (d, d) with maximum order of smoothness on a general domain is equal to the number of tensor–product B–spline basis functions, defined by only single knots in both directions, acting on the considered domain. A certain reasonable assumption on the configuration of the domain is required. This result is then generalized to the case of piecewise polynomial spaces, with the same smoothness properties mentioned above, defined on a nested sequence of domains, by providing a simple iterative procedure to define a basis for the bivariate hierarchical tensor–product spline space. Finally, it is observed that this construction corresponds to the classical definition of hierarchical B–spline bases.

Keywords: hierarchical B–splines, tensor–product basis, dimension, local refinement.

1 Introduction

Adaptive refinement of spline basis functions allows to localize changes in the control net so that the modification of a single control point will affect a limited region of the underlying geometric representation. Mesh refinement strategies constitute a fundamental component for the development of an effective approximation algorithm commonly used by standard surface reconstruction techniques. In the context of the numerical solution of partial differential equations, particular attention is currently devoted to this issue in connection with the emerging field of isogeometric analysis [3]. For this reason, refinement techniques which were originally introduced for standard geometric design applications, became the topic of recent studies, taking into account the dual requirements of geometry and analysis. The resulting novel perspective opened new path of research for the identification of geometric representations suitable for analysis which simultaneously satisfy the demand imposed by their use in the simulation framework and the accuracy of the geometrical model.

The extension of the isogeometric paradigm, originally introduced considering the NURBS model [11], with spline representations which allow local control of the refinement procedure has mainly focused on suitable applications [1, 6, 20] of the T–splines

*carlotta.giannelli@jku.at
†bert.juettler@jku.at

construction [22, 23]. Subsequently, alternative solutions based on the so–called polynomial splines over hierarchical T–meshes (PHT–splines) [4, 5, 14] and on hierarchical B–splines [7, 12] have also been considered [18, 24]. In this setting, the analytical point of view, which joins the geometric perspective, outlined the desire of characterizing the space spanned by the set of basis functions used to approximate the solution. This motivated investigations on the linear independence of T–splines blending functions [2, 16], discussion about the dimension of related spline spaces [17] and the corresponding nested nature of these T–spline spaces [15]. The hierarchical approach seems to be a valid solution to circumvent the weak points of T–splines identified by these studies (locality of the refinement [6], linear dependence associated with particular T–meshes [2], complexity of the enhanced refinement algorithm needed to ensure the linear independence of the blending functions [21]), and also the reduced regularity which characterizes PHT–splines (dimensions of spline spaces over T–meshes in the case that the degree is at least $2s + 1$ for splines with order of smoothness given by s were investigated in [4]).

The selection mechanism for the definition of a hierarchical B–splines basis introduced by Kraft in [12] by means of subsequent dyadic refinements ensures that

- hierarchical basis functions allows proper local refinement and are linearly independent (see Theorem 1 in [12]),
- the hierarchical B–spline basis is *weakly* stable, i.e. the stability constants depend on the number of hierarchical levels (see Theorem 3 in [12]).

Hierarchical B–splines have already been applied in several applications related to geometric modeling — see for example [8, 9, 10]. In addition, a hierarchical quasi–interpolant together with approximation algorithms and scattered data approximation and interpolation problems were also discussed in [12]. A more detailed analysis of the above mentioned topics can be found in [13]. The case of partly overlapping boundaries of the sub–domains which require further refinement and the nested nature of the hierarchical spline space, originally not properly discussed or outlined, have been considered in [24]. Even if Kraft also noted that spline surfaces defined by hierarchical B–splines of bi–degree d are C^{d-1} smooth (see Theorem 2 in [12] and item (b) of Theorem 2.2.1 in [13]), a general configuration of the hierarchical domains was not covered by the author. Only sub–domains with disjoint boundaries and defined as union of B–splines supports of the previous hierarchical level were considered.

The goal of the present paper is to make up this shortcoming by investigating dimensions and bases of hierarchical tensor–product B–spline spaces. The starting point of our study is a generalization of the dimension of bivariate tensor product polynomial spline spaces over more general domains than rectangular grids. By considering tensor–product spline functions with maximum order of smoothness, it turns out that the dimension formula on domains whose boundaries are piecewise linear closed curves (which satisfy a specific reasonable assumption) can be derived from the standard one related to rectangular grids (see, e.g., [19]) by including certain correction factors. This computation is then used to construct a basis for the bivariate hierarchical tensor–product spline space defined on a nested sequences of these domains. The hierarchical model allows complete

control of the refinement by using a spline hierarchy whose levels identifies subsequent levels of refinement. We consider an *increasingly nested* sequence of B–spline spaces $V^0 \subset V^1 \subset \ldots \subset V^{N-1}$, together with a *decreasingly nested* sequence of parametric domains $\Omega^0 \supseteq \Omega^1 \supseteq \ldots \supseteq \Omega^{N-1}$. The simple idea of the hierarchical spline model is based on a suitable correlation between these two nested structures: at each level ℓ, for $\ell = 0, 1, \ldots, N-1$, we iteratively select the basis functions from the underlying spline spaces V^ℓ, enlarged with respect to the one of the previous level, which only act on the current domain Ω^ℓ, selected to be refined. The local action of the refinement procedure is then immediately guaranteed by construction. Moreover, the local linear independence is inherited from the underlying B–spline bases, by subsequently discarding from the hierarchical basis the set of basis functions selected in the previous steps which also act only on the considered refined domain. By revisiting the classical construction of hierarchical tensor-product splines, we discuss dimensions and bases of hierarchically refined tensor-product B–spline spaces, showing how to construct bases which are non-negative and locally supported. In [24] the possibility of modifying these bases to form a partition of unity as well as their application for numerical simulation in isogeometric analysis are investigated.

The structure of the paper is as follows. After briefly introducing some preliminary notions in Section 2, we begin Section 3 by computing the dimension of the space of piecewise polynomials of degree (d, d) with maximum order of smoothness defined on a certain parametric domain, for then identifying a basis for this space in Section 4. This result is generalized to the case of spline spaces, with the same smoothness properties as before, defined on a nested sequence of these domains in Section 5. It is also shown that the classical hierarchical B–spline basis is a basis for this hierarchy of spaces. A simple refinement algorithm, based on the assumptions concerning the domain configuration needed to obtain the dimension formula mentioned above, is presented in Section 6. Finally, Section 7 concludes the paper.

2 Preliminaries

Let $\{V^\ell\}_{\ell=0,\ldots,N-1}$ be a sequence of N nested tensor–product spline spaces so that

$$V^\ell \subset V^{\ell+1},$$

for $\ell = 0, \ldots, N-2$. We assume the degree and smoothness at each level ℓ equal to (d, d) and $(d-1, d-1)$, respectively. Each spline space V^ℓ is spanned by a tensor–product B–spline basis T^ℓ defined on the two knot sequences $X^\ell = \{x_i^\ell\}_{i=0,\ldots,p}$ and $Y^\ell = \{y_j^\ell\}_{j=0,\ldots,q}$ containing the horizontal and vertical knots, respectively. These knot sequences, defined by only single knots at all levels, are also nested. In addition, we consider a finite sequence of N nested bounded open sets $\{\Omega^\ell\}_{\ell=0,\ldots,N-1}$ so that

$$\Omega^\ell \supseteq \Omega^{\ell+1}, \tag{1}$$

for $\ell = 0, \ldots, N-1$, with $\Omega^N = \emptyset$. At each level the boundary $\partial\Omega^\ell$ is aligned with the knot lines of $V^{\ell-1}$, $\ell = 1, \ldots, N-1$, while $\partial\Omega^0$ is aligned with the knot lines of V^0.

Moreover, we assume that

$$\Omega^0 \subseteq [x_d^0, x_{p-d}^0] \times [y_d^0, x_{q-d}^0].$$

and we consider the support of any function f when restricted to the domain Ω_0 by defining

$$\operatorname{supp} f = \{(x,y) : f(x,y) \neq 0 \ \wedge \ (x,y) \in \Omega^0\}.$$

The domain $R^\ell = \Omega^0 \setminus \Omega^{\ell+1}$ will be called a *ring* — even if it may not be ring–shaped — because, conceptually, it represents Ω^0 with an *hole* given by $\Omega^{\ell+1}$.

3 Dimension of bivariate tensor–product splines

In this section we derive the dimension formula of bivariate tensor–product splines on the ring R^ℓ for a fixed value of ℓ. The generalization of this result considering all the N levels of the hierarchy is then presented in Section 5.

3.1 Residual and boundary data

Given a fixed level ℓ, we consider the space S^ℓ of piecewise polynomials of degree (d,d) which are C^{d-1} smooth on the grid obtained by restricting the grid of the background space $V^\ell = \operatorname{span} T^\ell$ to $\Omega^0 \setminus \Omega^{\ell+1}$ for $\ell = 0, \ldots, N-1$, i.e.,

$$S^\ell = \left\{ f \in C^{d-1}(R^\ell) \wedge f \in V^\ell \right\}.$$

We denote with B and L the point sets composed by all the bottom and left edges which belong to R^ℓ. Let $B_1, \ldots, B_h$ and $L_1, \ldots, L_v$ be the horizontal and vertical elementary segments in which the bottom and left boundaries of the domain are subdivided. The bottom and left edges B and L can then be expressed as

$$B = \bigcup_{i=1}^{h} B_i, \qquad L = \bigcup_{j=1}^{v} L_j.$$

Definition 1. *By denoting with $\Pi^d(P)$ the space of polynomial functions of degree d over $P \subset \mathbb{R}^2$, we say that*

$$F = (b_1, \ldots, b_d, l_1, \ldots, l_d, r)$$

where

$$b_k : B \to \mathbb{R}, \qquad l_k : L \to \mathbb{R}, \qquad r : R^\ell \to \mathbb{R},$$

with $k = 1, \ldots, d$, so that, for all $i = 1, \ldots, h, j = 1, \ldots, v$ and for each cell c of the grid of R^ℓ,

$$b_k\big|_{B_i} \in \Pi^d(B_i), \quad l_k\big|_{L_j} \in \Pi^0(L_j), \quad \text{and} \quad r\big|_c \in \Pi^0(c),$$

is a vector of ***characteristic data****.*

A vector F of *characteristic* data is obtained from a function $f \in S^\ell$ by means of the characteristic operator M as

$$F = M(f) = (b_1, \ldots, b_d, l_1, \ldots, l_d, r)$$

where

$$\begin{aligned}
b_1(x,y) &= f(x,y)\big|_B\,, & l_1(x,y) &= \frac{\partial^d}{\partial y^d} f\big|_L \\
b_2(x,y) &= \frac{\partial}{\partial y} f(x,y)\big|_B\,, & l_2(x,y) &= \frac{\partial}{\partial x}\frac{\partial^d}{\partial y^d} f\big|_L\,, \\
&\vdots & &\vdots \\
b_d(x,y) &= \frac{\partial^{d-1}}{\partial y^{d-1}} f(x,y)\big|_B\,, & l_d(x,y) &= \frac{\partial^{d-1}}{\partial x^{d-1}}\frac{\partial^d}{\partial y^d} f\big|_L\,,
\end{aligned}$$

and

$$r(x,y) = \frac{\partial^d}{\partial x^d}\frac{\partial^d}{\partial y^d} f(x,y)\big|_c \quad \text{for each cell } c \text{ of the grid of } R^\ell.$$

Definition 2. *A vector F of characteristic data is said to be* ***feasible*** *if there exists $f \in S^\ell$ such that $F = M(f)$.*

Clearly, the set of feasible characteristic data forms a linear space. We can then relate this space to the spline space S^ℓ by means of the following proposition.

Proposition 3. *The mapping $M : S^\ell \to F$ between the spline space and the space of feasible characteristic data is an isomorphism of linear spaces.*

Proof. For any point $(x,y) \in R^\ell$, consider the rays with directions $(-1,0)$ and $(0,-1)$ and let $\hat{x} = \hat{x}(x,y)$, $\hat{y} = \hat{y}(x,y)$ be the horizontal and vertical coordinate of the intersection of these rays with the first vertical/horizontal boundary edge reached by them (see Figure 1). We can relate a function f in S^ℓ and a vector F of characteristic data in terms of the following differentiation/integration process. First, we execute d vertical differentiations

$$\begin{aligned}
f(x,y) &= b_1(x,\hat{y}) + \int_{\hat{y}}^{y} \frac{\partial}{\partial y} f(x,\eta)\mathrm{d}\eta, \\
\frac{\partial}{\partial y} f(x,y) &= b_2(x,\hat{y}) + \int_{\hat{y}}^{y} \frac{\partial^2}{\partial y^2} f(x,\eta)\mathrm{d}\eta, \\
&\vdots \\
\frac{\partial^{d-1}}{\partial y^{d-1}} f(x,y) &= b_d(x,\hat{y}) + \int_{\hat{y}}^{y} \frac{\partial^d}{\partial y^d} f(x,\eta)\mathrm{d}\eta,
\end{aligned} \tag{2}$$

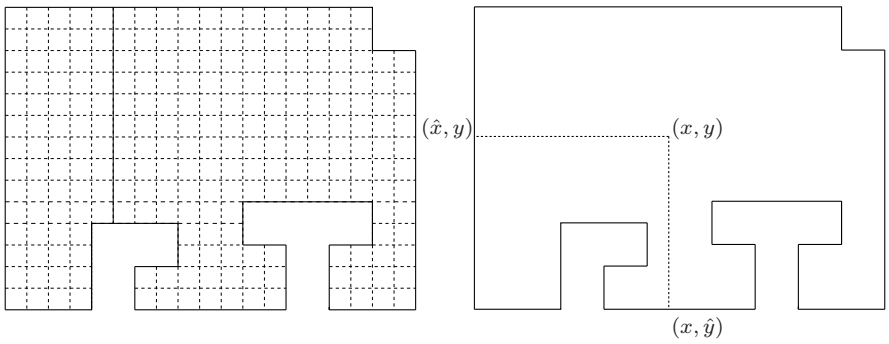

Figure 1: The ring $R^\ell = \Omega^0 \setminus \Omega^{\ell+1}$ and its grid (left) and the identification of $\hat{x} = \hat{x}(x, y)$ and $\hat{y} = \hat{y}(x, y)$ introduced in the proof of Proposition 3.

where $\hat{y}$ depends on (x, y), i.e., $\hat{y} = \hat{y}(x, y)$. Then, we continue with d horizontal differentiations

$$\begin{aligned}
\frac{\partial^d}{\partial y^d} f(x, y) &= l_1(\hat{x}, y) + \int_{\hat{x}}^{x} \frac{\partial}{\partial x} \frac{\partial^d}{\partial y^d} f(\xi, y) \mathrm{d}\xi, \\
\frac{\partial}{\partial x} \frac{\partial^d}{\partial y^d} f(x, y) &= l_2(\hat{x}, y) + \int_{\hat{x}}^{x} \frac{\partial^2}{\partial x^2} \frac{\partial^d}{\partial y^d} f(\xi, y) \mathrm{d}\xi, \\
&\vdots \\
\frac{\partial^{d-1}}{\partial x^{d-1}} \frac{\partial^d}{\partial y^d} f(x, y) &= l_d(\hat{x}, y) + \int_{\hat{x}}^{x} r(\xi, y) \mathrm{d}\xi,
\end{aligned} \tag{3}$$

where $\hat{x}$ depends on (x, y), i.e., $\hat{x} = \hat{x}(x, y)$. Hence, starting from a function $f \in S^\ell$, we may identify the associated feasible characteristic data F simply by means of Definition 2. On the other hand, starting with the set of constant values $r(x, y)$, which represent the derivative of order d in both directions, and with the following partial derivatives defined by the functions $b_1, \ldots, b_d$ and $l_1, \ldots, l_d$, we can reconstruct f by executing the above mentioned sequence of integrations in reverse order. □

3.2 Maximum horizontal components

We now need to specify the continuity conditions that a subset of characteristic data have to satisfy in order to be properly associated with a function f in S^ℓ by the mapping M as described in the previous Lemma. We may observe that the functions $b_1, \ldots, b_d$ are inter–dependent connected to each other (a C^{d-1} connection is required in anyone of the $h-1$ joint points along the horizontal direction), while the constants $l_1, \ldots, l_d$ are not (the C^{-1} connection is automatically achieved in anyone of the $v-1$ joint points along the vertical direction). In order to count the required conditions to impose we need the following definition.

Definition 4. *A connected horizontal component (HC) is a component of the bottom boundary composed of adjacent horizontal segments connected by only vertical edges. It is said to be a maximum HC (MHC) if it is not contained in any other HC.*

Each horizontal pair of adjacent elementary segments which belong to any MHC of the considered domain can be joined together according to one of the three cases shown in Figure 2 and indicated as flat join, step up join, and step down join.

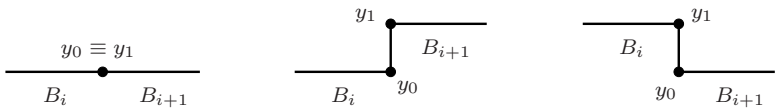

Figure 2: Joins between adjacent elementary segments: flat join (left), step up join (center), and step down join (right).

For any function $b_1, \ldots, b_d$, we may require the needed continuity in all the inner connection points of each MHC as a C^{d-1} join between

$$b_k\big|_{B_i} + v_k^i \quad \text{and} \quad b_k\big|_{B_{i+1}} + u_k^{i+1} \quad \text{at} \quad \pi(B_i) \cap \pi(B_{i+1}),$$

for $i = 1, \ldots, h-1$, where

$$v_k^i = 0, \quad u_k^i = 0, \qquad \text{in case of a flat join,} \tag{4}$$

$$v_k^i = \int_{y_0}^{y_1} \frac{\partial^{k-1}}{\partial y^{k-1}} f(x,\eta)\mathrm{d}\eta, \quad u_k^i = 0, \qquad \text{in case of a step up join,} \tag{5}$$

$$v_k^i = 0, \quad u_k^i = \int_{y_0}^{y_1} \frac{\partial^{k-1}}{\partial y^{k-1}} f(x,\eta)\mathrm{d}\eta, \qquad \text{in case of a step down join.} \tag{6}$$

The contribution – in terms of degrees of freedom – of all the MHCs which composed the bottom boundary of the given domain is then specified in the following Lemma.

Lemma 5. *The number of degrees of freedom associated with an MHC composed of e elementary horizontal segments is $d(e+d)$.*

Proof. For any function b_k, $k = 1, \ldots, d$,

$$b_k\big|_{B_1} + v_k^1 \quad \text{has to have a } C^{d-1} \text{ joint with} \quad b_k\big|_{B_2} + u_k^2 \quad \text{at} \quad \pi(B_1) \cap \pi(B_2),$$

$$b_k\big|_{B_2} + v_k^2 \quad \text{has to have a } C^{d-1} \text{ joint with} \quad b_k\big|_{B_3} + u_k^3 \quad \text{at} \quad \pi(B_2) \cap \pi(B_3),$$

and so on until

$$b_k\big|_{B_{e-1}} + v_k^{e-1} \quad \text{and} \quad b_k\big|_{B_e} + u_k^e \quad \text{at} \quad \pi(B_{e-1}) \cap \pi(B_e),$$

where u_k^i, v_k^i are defined by (4)–(6) for $i = 1, \ldots, e$. Since these relations only involve polynomial functions over the elementary segments $B_1, \ldots, B_e$, by using polynomial extrapolations we can equivalently expressed the above smoothness conditions as

$$c_k^{i-1} \quad \text{has to have a } C^{d-1} \text{ joint to} \quad c_k^i \quad \text{at} \quad \pi(B_{i-1}) \cap \pi(B_i)$$

for $i = 1, \ldots, e$, where

$$c_k^i = b_k\big|_{B_i} + \sum_{s=1}^{i-1} (u_k^{s+1} - v_k^s).$$

Hence, $\left(c_k^i\right)_{i=1,\ldots,e}$ form a C^{d-1} polynomial spline with $e + d$ degrees of freedom. $\square$

3.3 Construction of feasible characteristic data

In order to extend this result to more than one MHC we have to consider the following three types of MHCs (see also Figure 3).

(a) MHC not subject to boundary conditions;

(b) MHC with one boundary condition (on its left–hand or right–hand side);

(c) MHC with two boundary conditions.

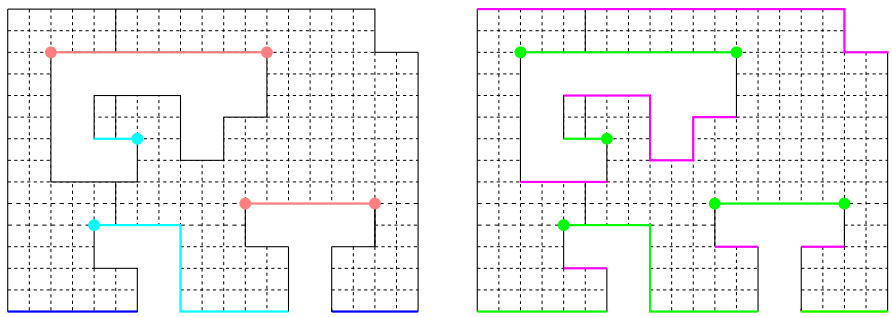

Figure 3: Classification of horizontal components: MHC not subject to boundary conditions (blue lines on the left), MHC with one boundary condition (cyan lines on the left), MHC with two boundary conditions (pink lines on the left). Also shown is the distinction between upper and lower MHCs (in magenta and green, respectively, on the right) introduced in Lemma 9.

We may observe that we can always split the bottom boundary of the domain in a unique sequence of MHCs. Moreover, as outlined by the following Lemma, at least one of the MHCs in this sequence is not subject to boundary conditions when considered in the vertical integration process described in the proof of Lemma 3. We will indicate an MHC of this type as *independent*. An independent MHC is obviously *left free* (no boundary conditions on left side) and *right free* (no boundary conditions on right side).

Lemma 6. *There always exists at least one independent MHC in the bottom boundary of the domain.*

Proof. Assume that no MHC is both left and right free. The leftmost corner of the bottom boundary of the domain is necessarily left free. Since the corresponding leftmost MHC cannot be also right free, the second leftmost MHC along the bottom boundary of the domain is also left free. Again, this second MHC cannot be also right free. We may then continue until we arrive at the rightmost MHC along the bottom boundary. However, this last MHC is necessarily also right free. This contradicts our assumption. □

An independent MHC imposes boundary conditions on other MHCs and its *shadow* (see Figure 4) decreases the domain. We are then able to describe a recursive algorithm to define feasible characteristic data for the integration process described in the proof of Lemma 3. We start from any of the independent MHCs which are present in the the considered domain. In view of the previous Lemma, at least one of them always exists.

Algorithm 7.

Input: a domain Ω, a constant value r for each cell of Ω, the functions l_k, $k = 1, \ldots, d$, on the vertical edges of the left boundary of Ω.

1. Evaluate, via equations (3),

$$\frac{\partial^{d-1}}{\partial x^{d-1}} \frac{\partial^d}{\partial y^d} f(x,y), \quad \ldots, \quad \frac{\partial}{\partial x} \frac{\partial^d}{\partial y^d} f(x,y), \quad \frac{\partial^d}{\partial y^d} f(x,y),$$

2. let Ω be the initial sub–domain not subject to boundary conditions;

3. select an independent MHC with respect to the current sub–domain;

4. for $k = d, \ldots, 1$

   (a) choose b_k on the selected MHC by taking into account possible boundary conditions of adjacent sub–domains (see below),

   (b) evaluate, via equations (2),

$$\frac{\partial^{k-1}}{\partial y^{k-1}} f(x,y),$$

   in its shadow and determine boundary conditions on adjacent MHCs which will be considered by neighboring sub–domains – see Figure 4;

5. reduce/split the current sub–domain by deleting the shadow of the selected MHC. This gives a set of sub-domains;

6. if the set of sub-domains is not empty then apply recursively step 3–5 to each sub-domain identified in step 5[1].

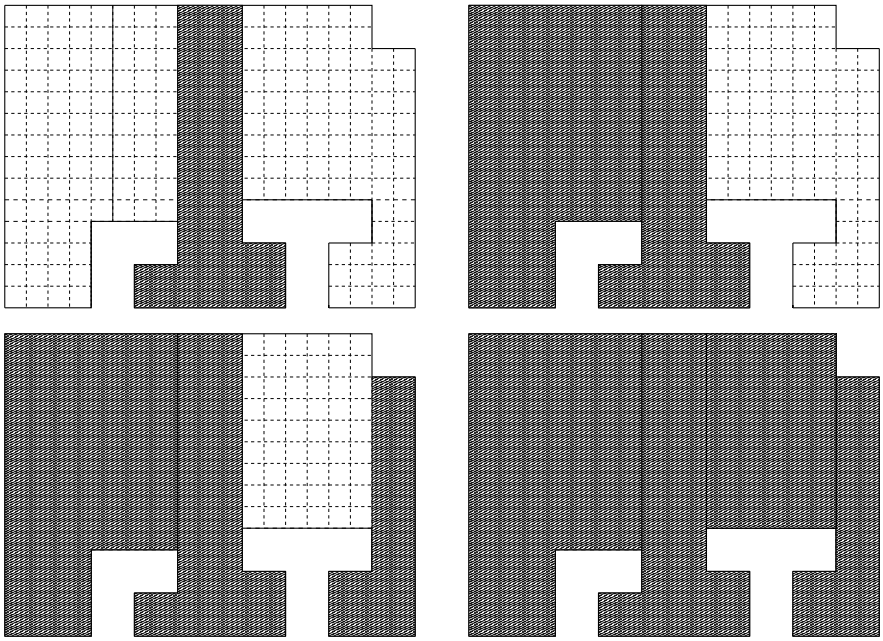

Figure 4: Boundary conditions computation with Algorithm 7. At each step the shadow of the selected independent MHC decreases, and eventually also splits, the domain.

Output: a set of feasible characteristic data and a corresponding spline function f on Ω.

We may observe that, for any MHC composed by e horizontal elementary segments, we have $e + d$ degrees of freedom (see the proof of Lemma 9 for the details). To impose the smoothness conditions as required by the integration process described above, when we consider a MHC with 2 boundary conditions, we have $e+d$ degrees of freedom minus a term of $2d$ given by the left and right boundary conditions. This leads to $e-d$ degrees of freedom, and then the length e of the MHC has to be greater or equal to d. We are then led to formulate the following assumption.

A0 The length (number of elementary horizontal segments) of any (lower) maximum horizontal component with two boundary conditions is at least d.

Lemma 8. *If assumption A0 is satisfied, algorithm 7 gives feasible characteristic data (boundary conditions) for the integration process described in the proof of Lemma 3.*

This can be proved easily by analyzing Algorithm 7.

3.4 Dimension formula

By firstly assuming the absence of holes, in view of the previous analysis, the bottom boundary is composed of:

[1]The values obtained in step 4 are used as boundary conditions on the remaining sub–domains.

1. one MHC of type (a), i.e., no boundary conditions – this is the one that, according to Lemma 6, always exists,
2. an arbitrary number of type (b) MHCs, i.e., one boundary condition,
3. a remaining arbitrary equal number of type (a) and (c) MHCs, i.e., zero and two boundary conditions, respectively.

Hence, the invariant property of the bottom boundary is that for each (c) there is always an (a). Let h_i be the number of elementary horizontal segments that compose one MHC. In the case of an MHC of type (a), the considered horizontal component contributes h_i+d degrees of freedom, while in case (b) we have to consider the d conditions to obtain a C^{d-1} join on its left or right boundary, leading to $h_i + d - d = h_i$. In case (c), instead, we have to take into account the d conditions to obtain a C^{d-1} join both on the left and right boundary of the MHC, leading to $h_i + d - 2d = h_i - d$. The total number of degrees of freedom associated with the bottom boundary of the domain is then always $\sum h_i + d$, as confirmed by the following Lemma.

Lemma 9. *Let C be the number of connected components of R^ℓ. If the considered domain does not exhibit holes, each one of the the d vertical integrations contributes*

$$\#\ \textit{of horizontal segments} + Cd$$

degrees of freedom.

Proof. We consider upper MHC and lower MHC (UMHC and LMHC) as shown on the right of Figure 3, and assume that the boundary is oriented counterclockwise. UMHC and LMHC alternate along the boundary. Between neighboring MHC, the boundary makes either a left turn or a right turn, both by 180 degrees. The total number of left turns is equal to the total number of right turns plus $2C$, because the boundary of any connected components of R^ℓ is a simple closed curve and the rotation index is therefore 1. We may observe that, if a LMHC follows

- a left turn, then there is no boundary condition on the left-hand side;
- a right turn, then there is one.

On the other hand, if a LMHC is followed by

- a left turn, then there is no boundary condition on its right-hand side;
- a right turn, then there is one.

For a LMHC with h_i edges, we have $(d+1)h_i - d(h_i - 1) = h_i + d$ degrees of freedom. If we have t LMHC, then will have $2t$ left turns or right turns, hence we have $t + C$ left turns and $t - C$ right turns. Each right turn imposes one boundary condition, hence it reduces the number of degrees of freedom by d. Summing up, we get

$$\sum_{i=1}^{t}(h_i + d) - (t - C)d = \sum_{i=1}^{t} h_i + td - td + Cd = \sum_{i=1}^{t} h_i + Cd$$

degrees of freedom. □

To relax the restriction related to the absence of holes and analyze how this influences the number of available degrees of freedom, we assume the boundaries of the holes are oriented counterclockwise as we already did for the boundary of the domain. Since the outer boundary of the hole is obviously inside the parametric domain, the distinction between lower and upper maximum connected horizontal component is now reversed – see again Figure 3. This implies that, in this case, a left turn before or after an MHC is the one which imposes a boundary condition on the left–hand side or right–hand side of the considered horizontal component. For an LMHC with h_i edges, we have $(d+1)h_i - d(h_i - 1) = h_i + d$ degrees of freedom as before. Again if we have t LMHC, then will have $2t$ left turns or right turns, hence we have $t+1$ left turns and $t-1$ right turns. Each left turn imposes one boundary condition, hence it reduces the number of degrees of freedom by d. Summing up we get

$$\sum_{i=1}^{t}(h_i + d) - (t+1)d = \sum_{i=1}^{t} h_i + td - td - d = \sum_{i=1}^{t} h_i - d$$

degrees of freedom.

Remark 10. *If the considered domain is characterized by one or more holes, for each of the d vertical integrations, any hole reduces the total degrees of freedom by d.*

Theorem 11. *If assumption A0 is satisfied, the dimension of the space S^ℓ is given by*

$$D = c + \frac{p}{2}d + Cd^2 - Hd^2, \tag{7}$$

where c is the number of cells of the domain, p the number of cells along its perimeter, C the number of connected components of the domain, and H the number of holes.

Proof. The first contribution simply arises from the c constant values for $r(x, y)$ that we associate to each cell of the considered domain. For each left edge considered in the d horizontal integrations, the involved partial derivatives $l_1, \ldots, l_d$ are constant with respect to the variable y. This leads to d times one degree of freedom for each vertical segment on the left boundary. The contribution to the available degrees of freedom which arises from the d vertical integrations is slightly more involved. However, we know from the previous analysis that is equal to $d(h + Cd - Hd)$ for a domain with C connected components and H holes. We may then conclude that the dimension of the space generated by the set of feasible characteristic data is

$$c + d\,(v + h + Cd - Hd) = c + d\frac{p}{2} + Cd^2 - Hd^2,$$

which directly leads to (7). □

Remark 12. *When $C = 1$ and $H = 0$, the value of D in (7) reduces to the dimension of bivariate tensor–product splines, defined by only single knots, on a rectangular grid, namely $D = (h + d)(v + d) = hv + (h + v)d + d^2 = c + \frac{p}{2}d + d^2$.*

4 Tensor–product spline bases

In this section we prove that the number of tensor product B–splines of degree (d, d) defined by only single knots in both directions and whose support overlaps a given domain is also equal to D. We focus again on the ring $R^\ell = \Omega^0 \setminus \Omega^{\ell+1}$ for a fixed level ℓ.

4.1 Offset to a domain

By considering the cells which belong to the the grid of R^ℓ or to the extension of this grid outside the boundary of this ring, let R^ℓ_k be the *offset region* at distance k from R^ℓ so that

$$R^\ell_0 = \{\text{cells inside } R^\ell \text{ which have at least one point along the boundary of } R^\ell\},$$
$$R^\ell_{k+1} = \{\text{cells} \not\subseteq R^\ell_k \text{ which have at least one point in common with } R^\ell_k\}.$$

We introduce the definitions of the *offset curve* to the ring R^ℓ at a certain distance and of its *length*.

Definition 13. *The* **offset curve** *to the ring R^ℓ is the piecewise linear curve defined as follows.*

(I) C_0, the offset curve at distance 0, is the boundary of the ring.

(II) Given the offset regions R^ℓ_k and R^ℓ_{k+1} for $k \in \mathbb{Z}^+$,

(a) R^ℓ admits offset at distance $k + \frac{1}{2}$ if any cell in R^ℓ_{k+1} is related to R^ℓ_k through one of the three connections shown in Figure 5; if this is the case, the offset curve at distance $k + \frac{1}{2}$, indicated as $C_{k+\frac{1}{2}}$, is the piecewise linear curve obtained by collecting together the contributions of any cell as shown in Figure 5;

(b) R^ℓ admits offset at distance $k + 1$ if the relationship between any cell in R^ℓ_{k+1} and R^ℓ_k falls into one of the three cases shown in Figure 6; if this is the case, the offset curve at distance $k + 1$, indicated as C_{k+1}, is the piecewise linear curve defined by the exterior boundary of R^ℓ_{k+1}.

If condition (a) or (b) in the above Definition is not satisfied, then the ring R^ℓ does not admit an offset at distance greater or equal to $k + \frac{1}{2}$ or $k + 1$, respectively. These conditions allow to guarantee that the piecewise linear curve which defines the offset at a certain distance is *self–intersection free*. This property is needed to ensure that the basis counting we are going to introduce is always feasible. Figure 7 shows a simple example of offset region and offset curve to the ring considered in Figure 3.

We may observe that, in our case of degree d and only single knots at all levels, the support of any B–spline is always composed by $(d + 1) \times (d + 1)$ elementary cells of the parametric grid. If the degree d is even, we can then identify each basis function with the central elementary cell of its support. When the degree d is odd, instead, we may identify each basis function with the center of its support. These naive *anchors* are

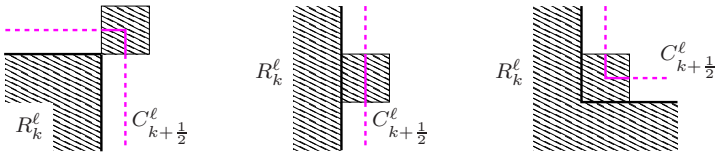

Figure 5: Admissible connections between a cell of R_{k+1}^ℓ and the offset region R_k^ℓ for defining the offset at distance $k+\frac{1}{2}$: one point (left), one side (center), and two adjacent sides (right). The piecewise linear contributions to the offset curve with respect to any of the three cases are also shown (magenta line).

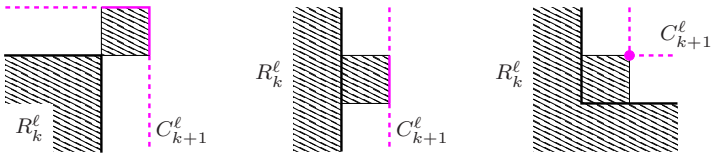

Figure 6: Admissible connections between a cell of R_{k+1}^ℓ and the offset region R_k^ℓ for defining the offset at distance $k+1$: two free sides (left), one free side (center), and one free point (right). The piecewise linear contributions to the offset curve with respect to the three admissible cases are also shown (magenta line).

called *odd* and *even* depending on the degree. They are shown in Figure 8 for the first four low degree cases.

Definition 14. *The* **length** *of an offset curve is the number of odd or even anchors that hit the offset itself.*

Let C_k^* be the offset at distance k to a connected component of the ring or to one of its hole. We define *extremal* corners of C_k^* the following four corners:

- the highest $\ulcorner$ and the lowest $\llcorner$ of the leftmost corners of C_k^*,
- the highest $\urcorner$ and the lowest $\lrcorner$ of the rightmost corners of C_k^*,

The remaining part of C_k^* is characterized by a certain number of left corners (L_c) and right corners (R_c) which, should increase or decrease, the length of C_k by two or one, in order to compute the length of C_{k+1} or $C_{k+\frac{1}{2}}$, respectively (see Figure 9). Using similar arguments as in the proof of Lemma 9, we may observe that the invariant property of a domain composed by C connected components, H holes, l left turns and r right turns, is that

$$l - r = 4C - 4H. \tag{8}$$

When C_k^* is the offset to a connected component of the boundary, assuming C_k^* to be counterclockwise oriented, the number of left corners always exceeds the number of right corners by 4 (see Figure 10). When C_k^* is the offset to a hole, in order to keep the

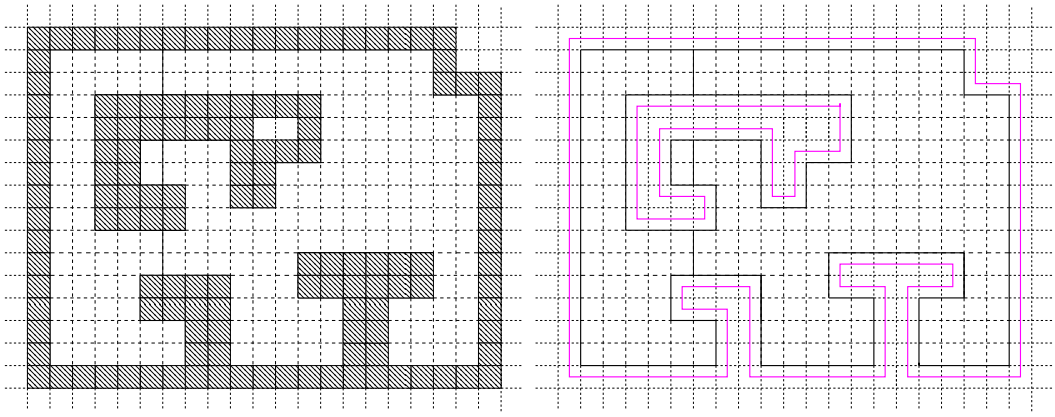

Figure 7: Offset region R_1^ℓ (hatched cells on the left) to the ring R^ℓ considered in Figure 3, and the corresponding offset curve $C_{\frac{1}{2}}$ (magenta line on the right). According to Definition 13, R^ℓ does not admit an offset at distance greater than $\frac{1}{2}$.

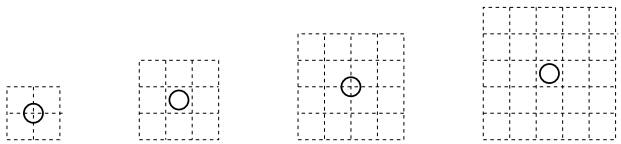

Figure 8: Basis functions representation in terms of odd ($d = 1, 3, \ldots$) and even ($d = 2, 4, \ldots$) anchors. From left to right: $d = 1, 2, 3, 4$.

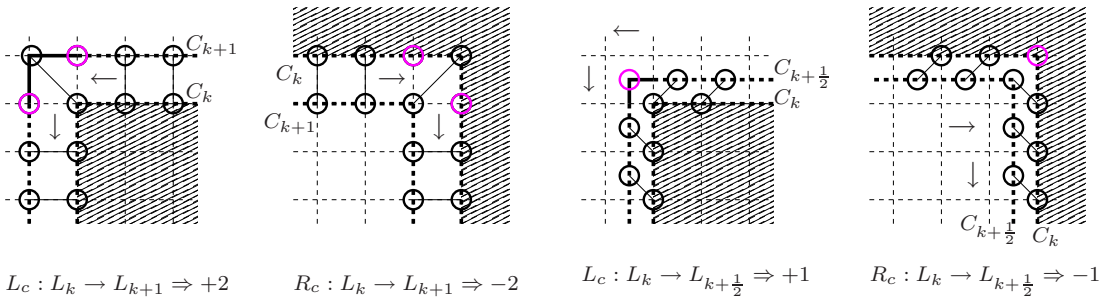

Figure 9: Classification of the corners along the offset curve and influence on the computation of the length according to Definition 14.

classification of the corners shown in Figure 9) still valid, we assume C_k^* to be clockwise oriented. In this case, the number of right corners always exceeds the number of left corners by 4 (see again Figure 10). In both cases the number 4 is given by the extremal corners of the piecewise linear curve. This explains the terms $+4C$ and $-4H$ in equations

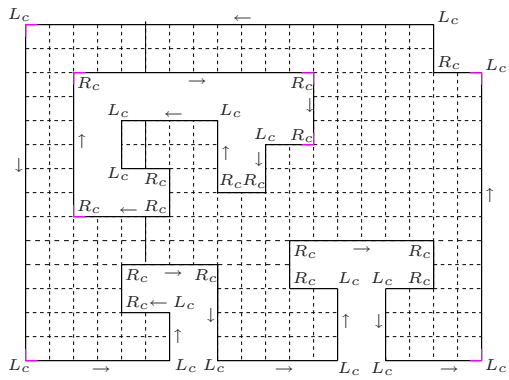

Figure 10: Corner classification for the ring of Figure 3: distinction between left (L_c) and right (R_c) corners. In this case: $C = H = 1$, $L_c = R_c = 16$, and $L_0 = L_{\frac{1}{2}} = 138$.

(8).

Lemma 15. *The length of the offset curve to the ring can be recursively computed as follows.*

(I) Base case: the length of C_0 is equal to the perimeter of the ring, i.e., $L_0 = p$.

(II) Recursive case: given the length of the offset curve at distance $k \in \mathbb{Z}^+$, indicated as L_k,

$$L_{k+\frac{1}{2}} = L_k + 4C - 4H, \qquad L_{k+1} = L_k + 8C - 8H. \tag{9}$$

Proof. In virtue of Figure 9, we have

$$L_{k+1} = L_k + 2(l - r), \qquad L_{k+\frac{1}{2}} = L_k + l - r.$$

By substituting (8) into the above relations, we obtain the two recursive equations in (9). □

We may observe that

$$L_k = p + 8k(C - H), \qquad L_{k+\frac{1}{2}} = p + 4(2k + 1)(C - H).$$

From the above relations we can compute the two sums

$$\sum_{k=0}^{n} L_k = (n + 1)p + 4n(n + 1)(C - H), \tag{10}$$

$$\sum_{k=0}^{n} L_{k+\frac{1}{2}} = (n + 1)p + 4(n + 1)^2(C - H), \tag{11}$$

which will be used in the proof of Theorem 17.

4.2 Basis functions enumeration

According to the previous analysis, the second assumption on the domain configuration is as follows.

A1 The ring R^ℓ admits offsets at distance less or equal to $(d-1)/2$.

This means that even degrees $d = 2n$ require offset at distances $n - \frac{1}{2}$, while odd degrees $d = 2n+1$ require offsets at distances n.

Let an *offset–segment* be the segment between two consecutive odd or even anchors along the offset curve at distance k or $k + \frac{1}{2}$, respectively, for any $k = 0, 1, \ldots$. We may observe that the offsetting procedure preserves the number of MHCs. This means that for any MHC along the ring R^ℓ there exists a corresponding MHC along each offset curve that the ring admits. Moreover,

- for any *lower* MHC along R^ℓ composed by n elementary horizontal segments, the corresponding MHC along the offset curve at distance $(d-1)/2$ is composed by $m = n - (d-1)$ offset–segments;
- for any *upper* MHC along R^ℓ composed by n elementary horizontal segments, the corresponding MHC along the offset curve at distance $(d-1)/2$ is composed by $m = n + (d-1)$ offset–segments.

Remark 16. *If the ring R^ℓ satisfies condition A1, then it also satisfies condition A0.*

Proof. If the domain admits offsets at distance less or equal to $(d-1)/2$, the number m of offset–segments along any MHC along the offset curve at distance $(d-1)/2$, which corresponds to a lower MHC along the boundary of R^ℓ, is at least 1. The number $n = m + d - 1$ of elementary horizontal segments which compose this lower MHC along R^ℓ is then greater or equal to d. □

We can formalize the counting of basis functions whose support has some non–empty intersections with the ring R^ℓ as follows.

Theorem 17. *The number of basis functions in the set*

$$T = \{\tau : \tau \in T^\ell \wedge \operatorname{supp} \tau \cap R^\ell \neq \emptyset\}$$

is equal to D (see Theorem 11) provided that assumption A1 holds. In this case, T is a basis of S^ℓ.

Proof. As shown in Figure 8 for the low degree cases, if the degree is even, i.e., $d = 2n$, we identify each basis function with the central elementary cell of its support. The total number of basis functions in T^ℓ whose support intersects with $\Omega^0 \setminus \Omega^{\ell+1}$ is given by

$$c + \sum_{k=0}^{n-1} L_{k+\frac{1}{2}} \tag{12}$$

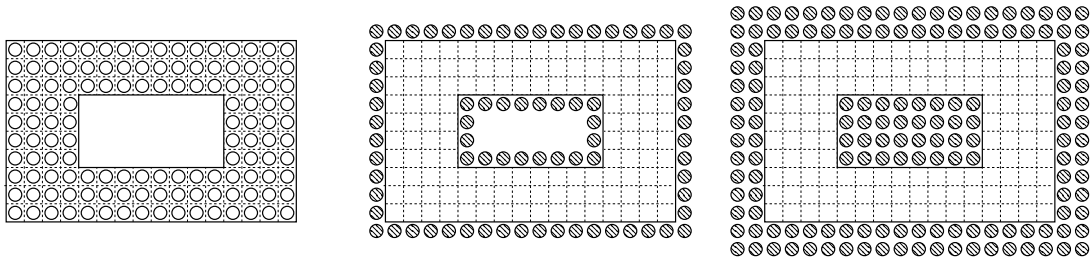

(a) First term in (12). (b) Second term in (12) for $d = 2$. (c) Second term in (12) for $d = 4$.

Figure 11: Number of tensor–product B–splines of degree 2 and 4 whose supports intersect the domain.

The first term counts all the basis function centered in a cell inside the domain. The second term instead counts each cell centered along offset curves at distances

$$\frac{1}{2}, 1 + \frac{1}{2}, \ldots, n - \frac{1}{2}.$$

The support of B–splines centered on the cells along these offset curves overlaps with the domain (see also Figure 11). By substituting (11) into (12), we obtain

$$c + np + 4n^2(C - H) = c + \frac{d}{2}p + 4\left(\frac{d}{2}\right)^2 (C - H) = D.$$

As already mentioned, when the degree d is odd, i.e., $d = 2n + 1$, we identify each basis function with the center of its support. The total number of basis functions in T^ℓ which intersect with $\Omega^0 \setminus \Omega^{\ell+1}$ is given by

$$\left(c - \frac{p}{2} + C - H\right) + \sum_{k=0}^{n} L_k \tag{13}$$

The first term counts all the basis function centered in a grid point inside the domain. The second term counts each cell centered along offset curves at distances

$$0, 1, \ldots, n,$$

i.e. that overlaps with the domain (see also Figure 12). By substituting (10) into (13), we obtain

$$c + \left(n + \frac{1}{2}\right) p + [4n(n + 1) + 1](C - H) = c + \frac{d}{2}p + 4\left(\frac{d}{2}\right)^2 (C - H) = D.$$

Obviously, the functions in T are linearly independent, hence they form a basis of S^ℓ. □

Figure 13 shows some admissible and non–admissible domain configurations.

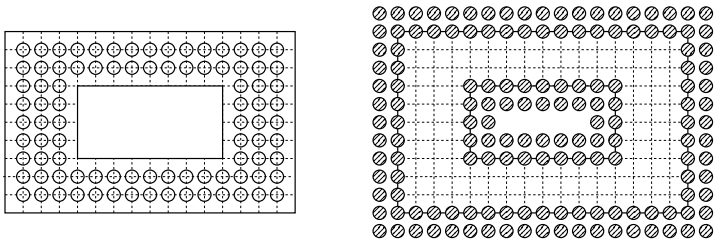

(a) First term in (13). (b) Second term in (13) for $d = 3$.

Figure 12: Number of tensor–product B–splines of degree 3 whose supports intersect the domain.

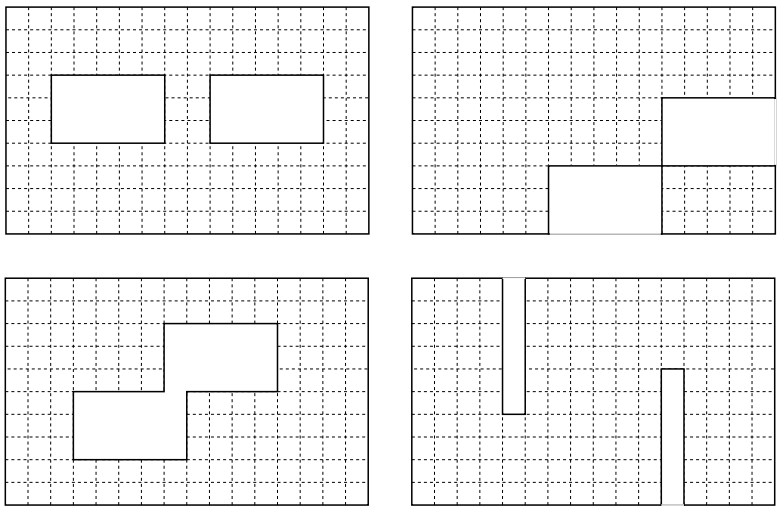

Figure 13: Examples of admissible (top) and non–admissible (bottom) domain configurations for $d = 2$.

5 The hierarchical space and its basis

Starting from the analysis of the previous section, we can now consider piecewise polynomial spaces of degree d and regularity $d-1$ defined on the nested sequence of domains introduced in (1).

5.1 Definition of the space

To generalize the previous results by considering all the levels of the hierarchy, we consider a function f in the space

$$W = \left\{ f \in C^{d-1}(\Omega^0) \wedge f\big|_{R^\ell} \in V^\ell, \ell = 0, \ldots, N-1 \right\}.$$

We assume that all rings $R^l = \Omega^0 \setminus \Omega^{\ell+1}$, for $\ell = 0, \dots, N-1$, satisfy the condition A1 introduced in Section 3 with respect to the grid of V^ℓ.

5.2 Hierarchical decomposition

The restriction of f to the ring $R^0 = \Omega^0 \setminus \Omega^1$ can be expressed as a linear combination of the basis functions in T^0 also restricted to this ring, namely

$$f\big|_{R^0} = \sum_{\tau \in T^0,\, \mathrm{supp}\,\tau \cap R^0 \neq \emptyset} c_\tau \tau\big|_{R^0}.$$

We can then define a corresponding function f^0, together with a residual function r^0, as

$$f^0 = \sum_{\tau \in T^0,\, \mathrm{supp}\,\tau \cap R^0 \neq \emptyset} c_\tau \tau, \qquad r^0 = f - f^0,$$

so that

$$f^0\big|_{R^0} = f\big|_{R^0}, \qquad r^0\big|_{R^0} = 0. \tag{14}$$

From the dimension formula derived in the previous sections, the restriction of r^0 to $R^1 = \Omega^0 \setminus \Omega^2$ can then be expressed as a linear combination of the basis functions in T^1 also restricted to this ring, namely

$$r^0\big|_{R^1} = \sum_{\tau \in T^1,\, \mathrm{supp}\,\tau \cap R^1 \neq \emptyset} c_\tau \tau\big|_{R^1}. \tag{15}$$

Let $\hat{\tau}$ be a basis function in T^1 for which $\mathrm{supp}\,\hat{\tau} \cap R^0 \neq \emptyset$. According to (14), when we consider the sum on the right–hand side of (15) restricted to a cell c of the grid associated to T^1 which also belongs to $\mathrm{supp}\,\hat{\tau} \cap R^0$, we obtain

$$\sum_{\tau \in T^1} c_\tau \tau\big|_c = 0.$$

All the basis function that are non–zero on the cell c are there locally linearly independent and the function $\hat{\tau}$ is one of them. This implies that $c_{\hat{\tau}} = 0$ and, consequently, relation (15) reduces to

$$r^0\big|_{R^1} = \sum_{\tau \in T^1,\, \mathrm{supp}\,\tau \cap \Omega^1 \setminus \Omega^2 \neq \emptyset,\, \mathrm{supp}\,\tau \subseteq \Omega^1} c_\tau \tau\big|_{R^1}.$$

Let f^1 and r^1 be

$$f^1 = \sum_{\tau \in T^1,\, \mathrm{supp}\,\tau \cap \Omega^1 \setminus \Omega^2 \neq \emptyset,\, \mathrm{supp}\,\tau \subseteq \Omega^1} c_\tau \tau, \qquad r^1 = f - f^1 - f^0.$$

They satisfy

$$\left(f^1 + f^0\right)\big|_{R^1} = f\big|_{R^1}, \qquad r^1\big|_{R^1} = 0. \tag{16}$$

As before, the restriction of r^1 to $R^2 = \Omega^0 \setminus \Omega^3$ can then be expressed as a linear combination of the basis functions in T^2 also restricted to this ring, namely

$$r^1\big|_{R^2} = \sum_{\tau \in T^2,\, \operatorname{supp}\tau \cap \Omega^2 \setminus \Omega^3 \neq \emptyset} c_\tau \tau\big|_{R^2}\,, \tag{17}$$

which, in view of (16), using similar arguments as before reduces to

$$r^1\big|_{R^2} = \sum_{\tau \in T^2,\, \operatorname{supp}\tau \cap \Omega^2 \setminus \Omega^3 \neq \emptyset,\, \operatorname{supp}\tau \subseteq \Omega^2} c_\tau \tau\big|_{R^2}\,. \tag{18}$$

Let f^2 and r^2 be

$$f^2 = \sum_{\tau \in T^2,\, \operatorname{supp}\tau \cap \Omega^2 \setminus \Omega^3 \neq \emptyset,\, \operatorname{supp}\tau \subseteq \Omega^2} c_\tau \tau, \qquad r^2 = f - f^2 - f^1 - f^0,$$

so that

$$\left(f^2 + f^1 + f^0\right)\big|_{R^2} = f\big|_{R^2}\,, \qquad r^2\big|_{R^2} = 0. \tag{19}$$

By iterating this argument for all the N levels of the hierarchy, we obtain

$$f^{N-1} = \sum_{\tau \in T^{N-1},\, \operatorname{supp}\tau \cap \Omega^{N-1} \setminus \Omega^N \neq \emptyset,\, \operatorname{supp}\tau \subseteq \Omega^{N-1}} c_\tau \tau,$$

and

$$r^{N-1} = f - f^{N-1} - \ldots - f^2 - f^1 - f^0,$$

so that

$$\left(f^{N-1} + \ldots + f^2 + f^1 + f^0\right)\big|_{R^{N-1}} = f\big|_{R^{N-1}}\,,$$

and, since $\Omega^N = \emptyset$, i.e., $R^{N-1} = \Omega^0 \setminus \Omega^N = \Omega^0$,

$$r^{N-1}\big|_{R^{N-1}} = r^{N-1}\big|_{\Omega^0} = 0.$$

This leads to

$$f = \sum_{i=0}^{N-1} f^\ell. \tag{20}$$

5.3 The Kraft basis

The selection mechanism for the underlying tensor product B–spline bases $T^0, \ldots, T^{N-1}$ introduced in Section 5.2, is summarized in the following definition, and generalizes the hierarchical B–spline basis originally introduced by Kraft in [12], where, for any hierarchical level, only sub–domains with disjoint boundaries defined as union of B–splines supports of the previous level were considered.

Definition 18. *The hierarchical basis $\mathcal{K}$ is defined as*

$$\mathcal{K} = \bigcup_{\ell=0}^{N-1} \left\{ \tau : \tau \in T^\ell \wedge \operatorname{supp}\tau \subseteq \Omega^\ell \wedge \operatorname{supp}\tau \not\subseteq \Omega^{\ell+1} \right\}.$$

At all levels ℓ, the support of the selected functions $\tau \in T^\ell$, which are newly added to the hierarchical basis $\mathcal{K}^\ell$, is entirely contained in the corresponding domain Ω^ℓ but not in $\Omega^{\ell+1}$. These basis functions satisfy the following two conditions

$$\operatorname{supp}\tau \cap R^{\ell-1} = \emptyset \quad \text{and} \quad \operatorname{supp}\tau \cap \left(\Omega^\ell \setminus \Omega^{\ell+1}\right) \neq \emptyset.$$

The refined domain $\Omega^{\ell+1}$ is then covered by basis functions $\tau \in T^{\ell+1}$. As proved in Theorem 19, the linear independence of the basis $\mathcal{K}$ is preserved by this construction.

Theorem 19. *If assumption A1 on the domain configuration holds, $\mathcal{K}$ is a basis of the space W.*

Proof. We have to prove that

1. any $f \in W$ belongs to the span of $\mathcal{K}$,
2. the basis functions in $\mathcal{K}$ are linearly independent, i.e.,

$$\sum_{\tau\in\mathcal{K}} d_\tau \tau = 0 \quad \Rightarrow \quad d_\tau = 0 \quad \forall \tau \in \mathcal{K}. \tag{21}$$

The first statement above follows directly from the hierarchical decomposition developed in Section 5.2. From equation (20) we obtain

$$\begin{aligned} f &= f^0 + f^1 + \ldots + f^{N-1} \\ &= \sum_{\tau\in T^0,\, \operatorname{supp}\tau\neq\emptyset} c_\tau \tau + \sum_{\tau\in T^1,\, \operatorname{supp}\tau\subseteq\Omega^1\setminus\Omega^2} c_\tau \tau + \ldots + \sum_{\tau\in T^{N-1},\, \operatorname{supp}\tau\subseteq\Omega^{N-1}} c_\tau \tau, \end{aligned}$$

where

$$f\,|_{R^\ell} = \sum_{i=0}^{\ell} f^i\,|_{R^\ell} \in V^\ell,$$

for $\ell = 0, \ldots, N-1$, and then $f \in \operatorname{span} W$.

To prove the second statement, we may observe that the sum in (21) can be rearranged by separating the basis functions of the hierarchical basis which come from different levels of the underlying sequence $\{T^\ell\}_{\ell=0,\ldots,N-1}$ as

$$\sum_{\tau\in\mathcal{K}\cap T^0} d_\tau \tau + \sum_{\tau\in\mathcal{K}\cap T^1} d_\tau \tau + \ldots + \sum_{\tau\in\mathcal{K}\cap T^{N-1}} d_\tau \tau = 0\,.$$

Considering all basis functions in the first sum of the above sequence, we may observe that these are the only non–zero functions on the ring defined by $\Omega^0 \setminus \Omega^1$. Now, since this set of basis function given by $\mathcal{K}\cap T^0$ is just a subset of T^0, the functions that it contains are locally linearly independent on $\Omega^0 \setminus \Omega^1$ and then, each coefficient d_τ associated to a basis function $\tau \in \mathcal{K} \cap T^0$ is zero. In the same way, the functions in $\mathcal{K} \cap T^1$ are linearly independent. Except for functions in $\mathcal{K} \cap T^0$, only these functions are non-zero on $\Omega^1 \setminus \Omega^2$. Again, in view of their local linear independence, this implies that $d_\tau = 0$ for $\tau \in \mathcal{K} \cap T^1$, and the same can be said for the next levels of the hierarchy. □

6 A simple refinement algorithm

We assume that, for any level, the number of cells in each direction, is a multiple of d. By denoting as *d–grid* of level ℓ the *aligned disjoint* boxes composed of $d \times d$ cells with respect to the grid of V^ℓ (see Figure 14), a naive algorithm to guarantee satisfaction of assumption A1 is based on the following observation.

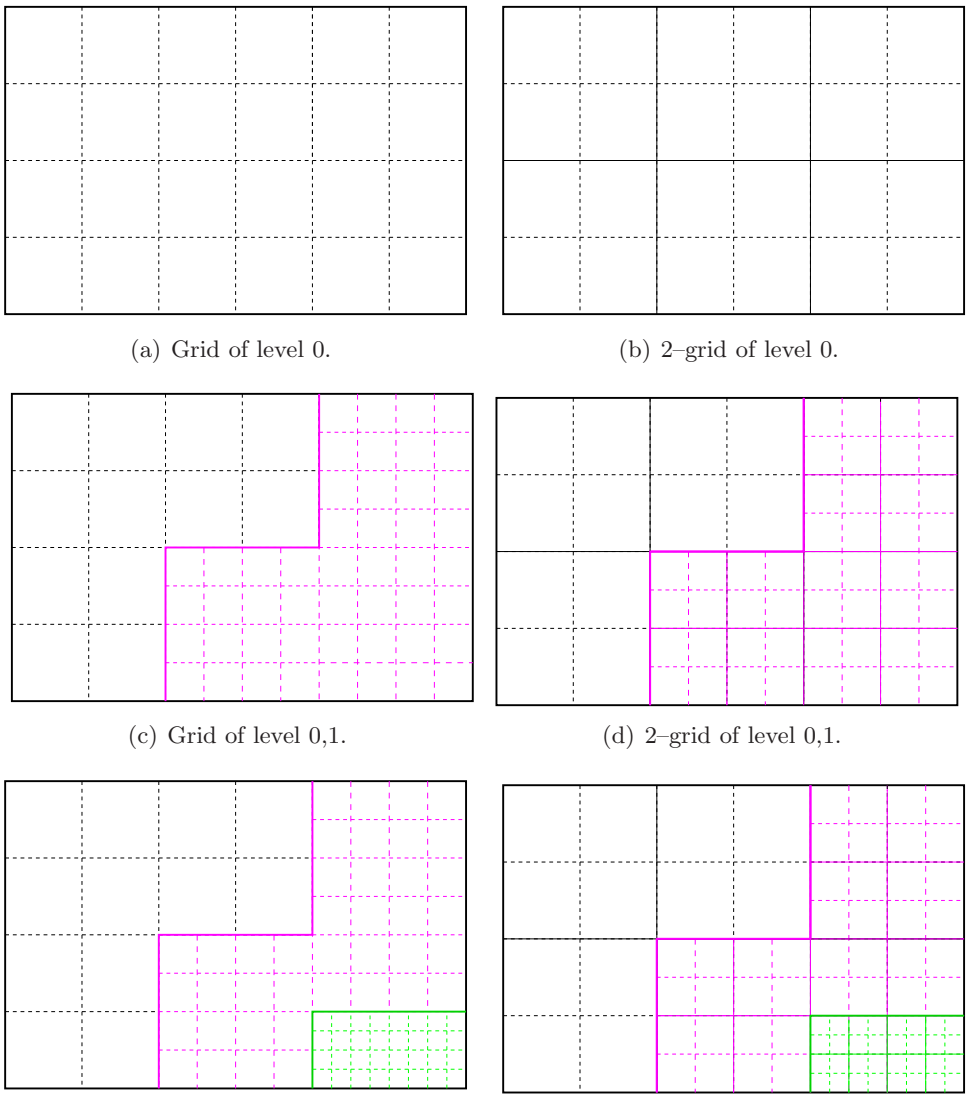

(a) Grid of level 0.

(b) 2–grid of level 0.

(c) Grid of level 0,1.

(d) 2–grid of level 0,1.

(e) Grid of level 0,1,2.

(f) 2–grid of level 0,1,2.

Figure 14: Grid and d–grid.

Remark 20. *If $\Omega^{\ell+1}$, for $\ell = 0, \ldots, N-2$, can be decomposed into a d–grid of level ℓ, then assumption A1 is satisfied.*

A simple refinement procedure based on the above observations may be summarized as follows.

Algorithm 21.

Input:

I1 A nested hierarchy of domains $\left\{\Omega^\ell\right\}_{\ell=0,\dots,N}$ so that

$$\Omega_0 \supseteq \Omega_1 \supseteq \dots \supseteq \Omega_N,$$

where each Ω^ℓ can be decomposed into a d–grid of level ℓ and $\Omega^N = \emptyset$;

I2 a subset $\Phi \subseteq \Omega^\ell$ of cells marked to be refined.

1. $\hat{\Omega}_0 = \Omega_0$;
2. for $\ell = 0, \dots, N-1$

$$\hat{\Omega}^{\ell+1} = \Omega^{\ell+1} \cup C$$

where C is the union of all the cells c which belong to the d–grid of level ℓ so that $c \cap \Phi \neq \emptyset$;

Output: the enlarged hierarchy of domains $\{\hat{\Omega}^\ell\}_{\ell=0,\dots,N}$ so that

$$\hat{\Omega}_0 \supseteq \hat{\Omega}_1 \supseteq \dots \supseteq \hat{\Omega}_N,$$

where each $\hat{\Omega}^\ell \supseteq \Omega^\ell$ is the union of *disjoint* boxes composed by $d \times d$ cells with respect to the grid of $V^{\ell-1}$.

Example 22. By considering the input data shown in Figure 15 with $d = 2$, the application of steps 2 of Algorithm 21 requires the three following iterations:

- $\ell = 0$: enlargement of Ω_1 with 1 box composed by 2×2 cells with respect to the grid of V^0 to define $\hat{\Omega}^1$, see Figure 16 (a)–(b);
- $\ell = 1$: enlargement of Ω_2 with 2 boxes composed by 2×2 cells with respect to the grid of V^1 to define $\hat{\Omega}^2$, see Figure 16 (c)–(d);
- $\ell = 2$: definition of $\hat{\Omega}_3$ as union of 2 disjoint boxes composed by 2×2 cells with respect to the grid of V^2, see Figure 16 (e)–(f).

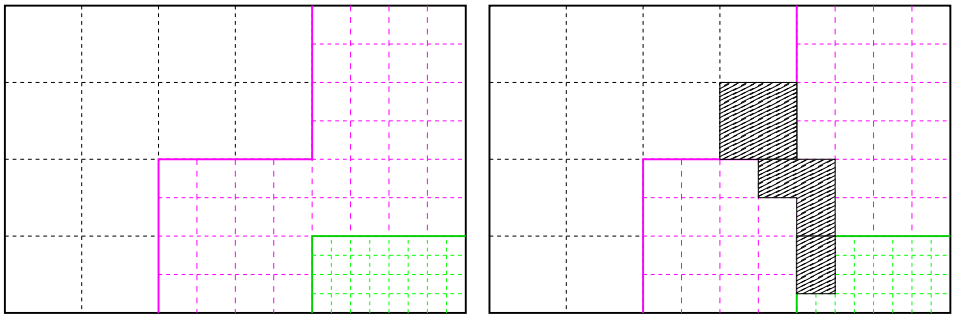

(a) $\{\Omega^\ell\}_{\ell=0,1,2,3}$ with $\Omega^3 = \emptyset$. (b) Area selected to be refined: Φ.

Figure 15: Input data for Algorithm 21 considered in Example 22. The three domains Ω^0 (black), Ω^1 (magenta), Ω^2 (green) on the left, must be refined according to the subset Φ of marked cells shown on the right (hatched region).

7 Closure

The dimension of smooth bivariate hierarchical tensor–product B–spline spaces defined on general domains has been identified. A detailed analysis of the admissible domain configurations covered by the proposed analysis has been presented, leading to the formulation of assumption A1. This includes a simple algorithm which ensures the repeated fulfillment of these condition during the refinement procedure. The development of a more sophisticated algorithm based on weaker assumptions on the domain configuration which allows anyway to satisfy condition A1 may be the subject of further studies.

The hierarchical basis can be suitably modified in order to define a piecewise polynomial basis which is non–negative and consists of locally supported basis functions which also form a partition of unity. The possibility of modifying the basis functions to define a normalized *weighted* basis is discussed in [24].

Acknowledgments

The research leading to these results has received funding from the European Union Seventh Framework Programme (FP7/2007-2013) under grant agreements n°214584 (SAGA) and n°272089 (PARADISE).

References

[1] Y. Bazilevs, V. M. Calo, J. A. Cottrell, J. Evans, T. J. R. Hughes, S. Lipton, M. A. Scott, and T. W. Sederberg. Isogeometric Analysis using T–splines. *Computer Methods in Applied Mechanics and Engineering*, 199:229–263, 2010.

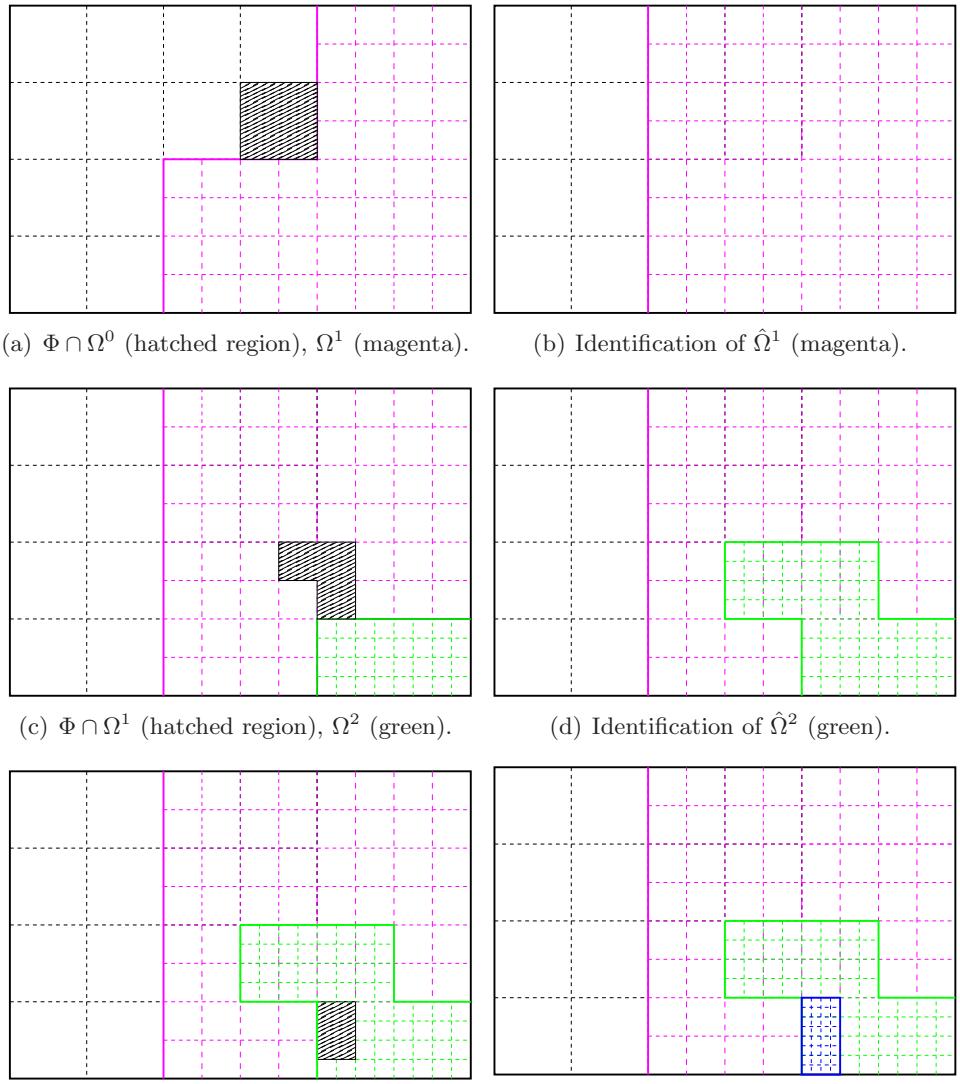

(a) $\Phi \cap \Omega^0$ (hatched region), Ω^1 (magenta).

(b) Identification of $\hat{\Omega}^1$ (magenta).

(c) $\Phi \cap \Omega^1$ (hatched region), Ω^2 (green).

(d) Identification of $\hat{\Omega}^2$ (green).

(e) $\Phi \cap \Omega^2$ (hatched region), $\Omega^3 = \emptyset$.

(f) Identification of $\hat{\Omega}^3$ (blue).

Figure 16: The three steps required by Algorithm 21 for constructing the enlarged sequence $\{\hat{\Omega}^\ell\}$, $\ell = 0, 1, 2, 3$ starting from the input data of Figure 15. Note that the coarsest level remains unchanged: $\hat{\Omega}^0 = \Omega^0$ (black grid).

[2] A. Buffa, D. Cho, and G. Sangalli. Linear independence of the T–spline blending functions associated with some particular T–meshes. *Computer Methods in Applied Mechanics and Engineering*, 199:1437–1445, 2010.

[3] J. A. Cottrell, T. J. R. Hughes, and Y. Bazilevs. *Isogeometric Analysis: Toward Integration of CAD and FEA*. John Wiley & Sons, 2009.

[4] J. Deng, F. Chen, and Y. Feng. Dimensions of spline spaces over T–meshes. *Journal of Computational and Applied Mathematics*, 194:267–283, 2006.

[5] J. Deng, F. Chen, X. Li, Ch. Hu, Tong W., Z. Yang, and Y. Feng. Polynomial splines over hierarchical T–meshes. *Graphical Models*, 70:76–86, 2008.

[6] M. R. Dörfel, B. Jüttler, and B. Simeon. Adaptive isogeometric analysis by local h-refinement with T–splines. *Computer Methods in Applied Mechanics and Engineering*, 199:264–275, 2010.

[7] D. R. Forsey and R. H. Bartels. Hierarchical B–spline refinement. *Computer Graphics*, 22:205–212, 1988.

[8] D. R. Forsey and R. H. Bartels. Surface fitting with hierarchical splines. *ACM Transactions on Graphics*, 14:134–161, 1995.

[9] D. R. Forsey and Wong D. Multiresolution surface reconstruction for hierarchical B–splines. In *Graphics Interface*, pages 57–64, 1998.

[10] G. Greiner and K. Hormann. Interpolating and approximating scattered 3D–data with hierarchical tensor product B–splines. In A. Le Méhauté, C. Rabut, and L. L. Schumaker, editors, *Surface Fitting and Multiresolution Methods*, Innovations in Applied Mathematics, pages 163–172. Vanderbilt University Press, Nashville, TN, 1997.

[11] T. J. R. Hughes, J. A. Cottrell, and Y. Bazilevs. Isogeometric analysis: CAD, finite elements, NURBS, exact geometry and mesh refinement. *Computer Methods in Applied Mechanics and Engineering*, 194:4135–4195, 2005.

[12] R. Kraft. Adaptive and linearly independent multilevel B–splines. In A. Le Méhauteé, C. Rabut, and L. L. Schumaker, editors, *Surface Fitting and Mulitresolution Methods*, pages 209–218. Vanderbilt University Press, Nashville, 1997.

[13] R. Kraft. *Adaptive und linear unabhängige Multilevel B–Splines und ihre Anwendungen*. PhD thesis, Universität Stuttgart, 1998.

[14] X. Li, J. Deng, and F. Chen. Polynomial splines over general T-meshes. *Visual Computer*, 26:277–286, 2010.

[15] X. Li and M. A. Scott. On the nesting behavior of T–splines. Technical Report 11-13, ICES, 2011.

[16] X. Li, J. Zheng, T. W. Sederberg, T. J. R. Hughes, and M. A. Scott. On linear independence of T–splines. Technical Report 10-40, ICES, 2010.

[17] B. Mourrain. On the dimension of spline spaces on planar T–subdivisions. 2010. URL `http://hal.inria.fr/inria-00533187/en`.

[18] N. Nguyen-Thanh, H. Nguyen-Xuan, S. P. A. Bordas, and T. Rabczuk. Isogeometric analysis using polynomial splines over hierarchical T-meshes for two-dimensional elastic solids. *Computer Methods in Applied Mechanics and Engineering*, 200:1892–1908, 2011.

[19] L. Schumaker. *Spline functions: basic theory.* Cambridge University Press, 2007.

[20] M. A. Scott, M. J. Borden, C. V. Verhoosel, T. W. Sederberg, and T. J. R. Hughes. Isogeometric finite element data structures based on Bézier extraction of T-splines. Technical Report 10-45, ICES, 2010.

[21] M. A. Scott, X. Li, T. W. Sederberg, and T. J. R. Hughes. Local refinement of analysis-suitable T-splines. Technical Report 11-06, ICES, 2011.

[22] T. W. Sederberg, D. L. Cardon, G. T. Finnigan, N. S. North, J. Zheng, and T. Lyche. T-spline simplification and local refinement. *ACM Transactions on Graphics*, 23:276 – 283, 2004.

[23] T. W. Sederberg, J. Zheng, A. Bakenov, and A. Nasri. T-splines and T-NURCCS. *ACM Transactions on Graphics*, 22:477–484, 2003.

[24] A.-V. Vuong, C. Giannelli, B. Jüttler, and B. Simeon. A hierarchical approach to adaptive local refinement in isogeometric analysis. Technical report, 2011. FB Mathematik, TU Kaiserlautern.

Technical Reports of the Doctoral Program

"Computational Mathematics"

2011

2011-01 S. Takacs, W. Zulehner: *Convergence Analysis of Multigrid Methods with Collective Point Smoothers for Optimal Control Problems* February 2011. Eds.: U. Langer, J. Schicho

2011-02 L.X.Châu Ngô: *Finding rational solutions of rational systems of autonomous ODEs* February 2011. Eds.: F. Winkler, P. Paule

2011-03 C.G. Raab: *Using Gröbner Bases for Finding the Logarithmic Part of the Integral of Transcendental Functions* February 2011. Eds.: P. Paule, V. Pillwein

2011-04 S.K. Kleiss, B. Jüttler, W. Zulehner: *Enhancing Isogeometric Analysis by a Finite Element-Based Local Refinement Strategy* April 2011. Eds.: U. Langer, J. Schicho

2011-05 M.T. Khan: *A Type Checker for MiniMaple* April 2011. Eds.: W. Schreiner, F. Winkler

2011-06 M. Kolmbauer: *Existence and Uniqueness of Eddy current problems in bounded and unbounded domains* May 2011. Eds.: U. Langer, V. Pillwein

2011-07 M. Kolmbauer, U. Langer: *A Robust Preconditioned-MinRes-Solver for Distributed Time-Periodic Eddy Current Optimal Control Problems* May 2011. Eds.: R. Ramlau, W. Zulehner

2011-08 M. Wiesinger-Widi: *Sylvester Matrix and GCD for Several Univariate Polynomials* May 2011. Eds.: B. Buchberger, V. Pillwein

2011-09 M. Wiesinger-Widi: *Towards Computing a Gröbner Basis of a Polynomial Ideal over a Field by Using Matrix Triangularization* May 2011. Eds.: B. Buchberger, V. Pillwein

2011-10 M. Kollmann, M. Kolmbauer: *A preconditioned MinRes solver for time-periodic parabolic optimal control problems* August 2011. Eds.: U. Langer, V. Pillwein

2011-11 C. Giannelli, B. Jüttler: *Bases and dimensions of bivariate hierarchical tensor–product splines* October 2011. Eds.: U. Langer, J. Schicho

The complete list since 2009 can be found at
`https://www.dk-compmath.jku.at/publications/`

Doctoral Program
"Computational Mathematics"

Director:

Prof. Dr. Peter Paule
Research Institute for Symbolic Computation

Deputy Director:

Prof. Dr. Bert Jüttler
Institute of Applied Geometry

Address:

Johannes Kepler University Linz
Doctoral Program "Computational Mathematics"
Altenbergerstr. 69
A-4040 Linz
Austria
Tel.: ++43 732-2468-7174

E-Mail:

office@dk-compmath.jku.at

Homepage:

http://www.dk-compmath.jku.at

Submissions to the DK-Report Series are sent to two members of the Editorial Board who communicate their decision to the Managing Editor.